*Geochimica et Cosmochimica Acta* Vol. 54, pp. 3461–3473


0016-7037/90/$3.00 + .00

# Primary and diagenetic controls of isotopic compositions of iron-formation carbonates

ALAN J. KAUFMAN,[1] J. M. HAYES,[1] and C. KLEIN[2]

[1]Biogeochemical Laboratories, Departments of Geological Sciences and of Chemistry, Indiana University, Bloomington, IN 47405-5101, USA

[2]Department of Geology, University of New Mexico, Albuquerque, NM 87131, USA

(*Received January* 4, 1990; *accepted in revised form October* 3, 1990)

**Abstract**—Mineralogic, chemical, and isotopic compositions have been determined for 97 carbonate microbands in five core segments from the early Proterozoic (2.5 Ga) Dales Gorge Member of the Brockman Iron Formation, Hamersley Basin, Western Australia. Samples were obtained both from banded iron-formation (BIF) macrobands 9–12 at Paraburdoo, on the southern margin of the basin, and from BIF macroband 13 at Wittenoom, 130 km NW. At Paraburdoo, oxygen-isotopic compositions of coexisting chert and magnetite microbands were measured and indicated final equilibration temperatures ranging from 60–160°C. This range is consistent with observed mineral assemblages and indicates a considerable temperature gradient across the basin (cf. T ~ 300°C at Wittenoom; BECKER and CLAYTON, 1976). Carbon-isotopic compositions of carbonates are near −7‰ vs. PDB at Paraburdoo and −10.5‰ at Wittenoom, but the greater isotopic depletion at Wittenoom appears related to primary or diagenetic processes, not metamorphism. Contents of organic carbon are consistently low. Isotopic depletion is roughly correlated with iron abundance and, together with petrographic observations and chemical balances, is consistent with the model of BIF deposition introduced by BEUKES et al. (1990): primary siderite ($\delta \sim -5$‰) precipitated from an anoxic water column depleted in $^{13}C$; additional depletion of $^{13}C$ is associated with coprecipitation of iron oxides and organic carbon.

Oxygen-isotopic abundances of microbanded carbonates are similar to those of under- and overlying massive marine carbonates, ranging from 17.6 to 21.0‰ vs. SMOW (−9.6 to −12.9‰ vs. PDB). Millimeter-scale variations in abundances of $^{13}C$ and $^{18}O$ are associated with diagenetic replacement of primary siderite by secondary ankerite and/or magnetite. It is shown that these isotopic variations cannot result from mineral-dependent fractionations, metamorphism, or the influence of large volumes of water in an open system.

## INTRODUCTION

ISOTOPIC AND MINERALOGIC compositions of microbanded carbonates and cherts in the early Proterozoic (2.5 Ga) Dales Gorge Member, Brockman Iron Formation, Hamersley Group, Western Australia, were investigated in order to obtain a better understanding of the formation of these deposits. We focused our studies on the microbands, which have been interpreted as varves analogous to those noted in evaporite formations (e.g., Permian Castile Formation, West Texas) that resulted from annual chemical variations in the depositional basin (TRENDALL and BLOCKLEY, 1970; TRENDALL, 1973; GARRELS, 1987). Carbonate is present in unmetamorphosed banded iron-formations (BIF) as ankerite or as siderite containing minor Ca or Mg (JAMES, 1955; DIMROTH, 1968; DIMROTH and CHAUVEL, 1973; TRENDALL and BLOCKLEY, 1970; AYRES, 1972; KLEIN, 1974; KLEIN and BRICKER, 1977; EWERS; 1980, 1983; EWERS and MORRIS, 1981; KLEIN and BEUKES, 1989; BEUKES et al., 1990). Variations in the isotopic compositions of these carbonates might reflect

1) variations in the chemical composition of primary and diagenetic carbonates,
2) primary changes in the isotopic composition of the water column beneath which the BIF formed,
3) oxygen-isotopic exchange between carbonates and coexisting mineral phases,
4) post depositional thermal processes (i.e., iron-dependent oxidation of organic carbon, PERRY et al., 1973).

The Dales Gorge Member (approximately 160 m thickness) is the lowermost unit of the Brockman Iron Formation in the Hamersley Group (Fig. 1). Three scales of banding (termed macro-, meso-, and microbanding) are evident (TRENDALL and BLOCKLEY, 1970). Macrobands are designated BIF 0 through BIF 16 and S 1 through S 16, respectively, corresponding to the oxide- and silicate-types of iron-formation as defined by JAMES (1954). Within the macrobands are centimeter-sized mesobands and millimeter-sized microbands of iron oxides, iron silicates, iron carbonates, and chert, with minor amounts of pyrite and organic carbon.

Studies of elemental abundances support the assumption that primary chemical precipitates were similar across the depositional basin (TRENDALL and PEPPER, 1977; EWERS and MORRIS, 1981); however, variations in mineralogic assemblages suggest increasing metamorphic grade from Paraburdoo to Wittenoom (EWERS and MORRIS, 1981; see Fig. 1 for locations). From oxygen-isotopic analyses of coexisting quartz, magnetite, and siderite in mesoband samples from Wittenoom, BECKER and CLAYTON (1976) concluded that maximum burial temperatures ranged from 270 to 310°C. Differences in $^{18}O$ abundances between coexisting quartz and magnetite were shown to vary widely over short distances, a feature attributed to local variations in permeability of the sediments. Isotopic temperatures are inconsistent with temperatures determined from mineralogic phase equilibria which, in nearby samples from the Dales Gorge Member and

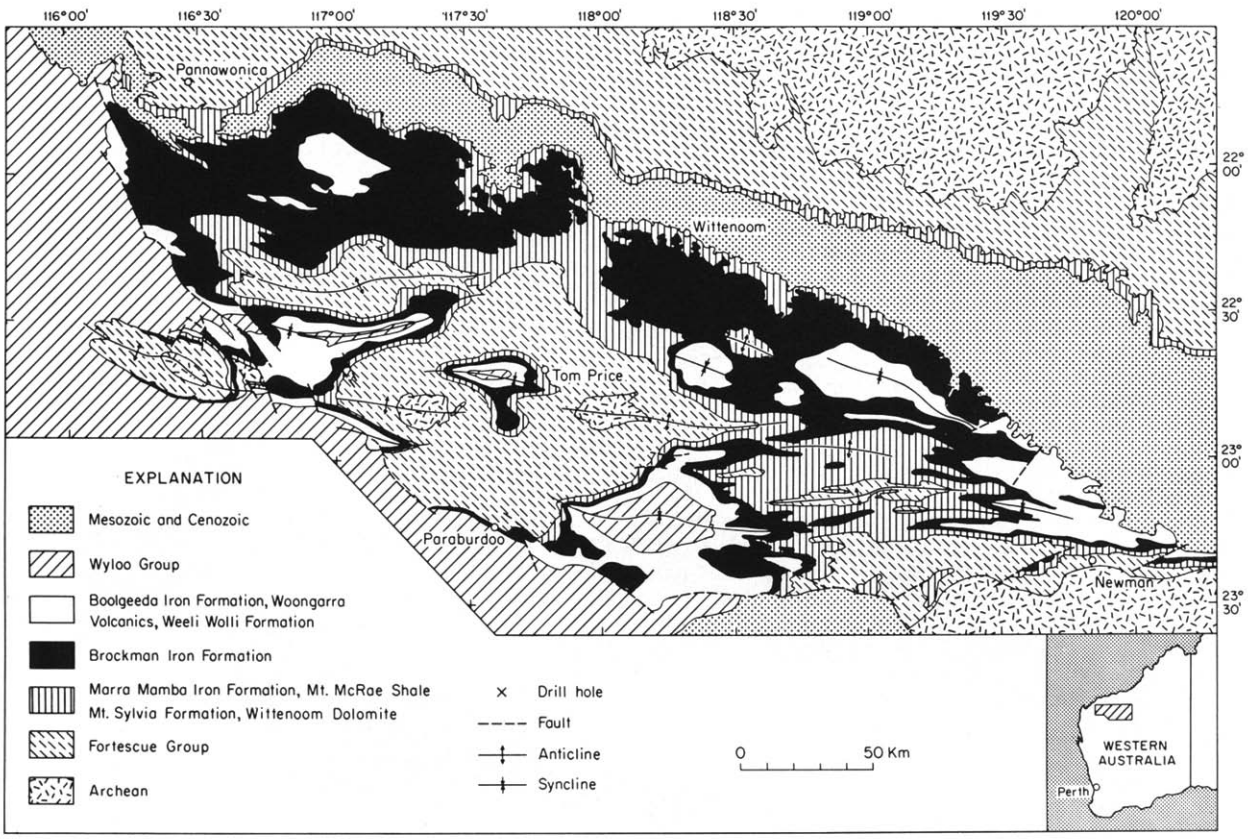


FIG. 1. Distribution of the Brockman Iron Formation in the Hamersley Range (after MACLEOD, 1966). The locations of Wittenoom and Paraburdoo, separated by approximately 180 km, are shown.

the underlying Marra Mamba Iron Formation, range as low as 120 ± 40°C (MIYANO, 1987).

Carbon-isotopic analyses by BECKER and CLAYTON (1972) of mesobanded carbonates revealed a general depletion in $^{13}C$ relative to early Proterozoic non-iron-rich carbonates. In a later study, BAUR et al. (1985) analyzed microbanded carbonates from the underlying Marra Mamba Iron Formation and Bruno's Band of the Mt. Sylvia Formation, but generally avoided the Dales Gorge Member because its extensive silicification made fine-scale sampling difficult. Microbanded carbonates were found to be depleted in $^{13}C$ (relative to massive and stromatolitic carbonates deposited in the same basin), and isotopic abundances of $^{13}C$ and $^{18}O$ varied significantly between successive microbands, with depletions in both isotopes being correlated with increased concentrations of iron (BAUR et al., 1985). In the present study, improved microdrilling techniques have allowed parallel analyses of both carbonate and chert microbands in the Dales Gorge Member. Isotopic, chemical, and mineralogic variations in microbanded carbonates, cherts, and coexisting minerals in four core segments from Paraburdoo and one from Wittenoom were investigated to determine

1) whether millimeter-scale variations reflect primary or secondary processes related to the genesis of the BIF,
2) whether variations across the basin are a function of prograde metamorphism (cf. EWERS and MORRIS, 1981).

## MATERIALS AND METHODS

### Sample Collection and Preparation

Core material was collected by C.K. and J.M.H. from BIF macrobands 9–12 at Paraburdoo (drillhole 75-1) and BIF and S macrobands 11 and 13 from the type section at Wittenoom (drillhole EC 10). Short core sections (5–10 cm) particularly rich in carbonate microbands were chosen from these intervals for detailed sampling and isotopic analysis of carbonates. Thin, flat slabs were cut from one face of the core, and polished thin sections for electron-probe microanalysis were prepared from the newly formed, mirror-image cut face. Additionally, thin sections were prepared from remaining slabs for petrographic analysis and staining to determine bulk carbonate mineralogy of each microband. Microsampling of carbonate and chert laminae within the flat slabs was carried out by binocular microscopic observation and fine-scale manipulation of a low-speed drill using either a 0.75- or 1.00-mm diameter steel mandrel tipped with synthetic diamonds. Although the diameter of the diamond-drill was generally greater than the width of the laminae, care was taken to avoid sampling the same mineral from two microbands simultaneously. The resulting fine powder was collected and split into two approximately equivalent portions for subsequent isotopic analysis. Drill bits, flat core sections, and the microsampling stage were cleaned after each microband was drilled. Residues of thin-section billets, representative of the full length of each core segment, were crushed to provide whole-rock powder samples.

### Analytical Methods

Carbon dioxide was evolved from carbonates by treatment with $H_3PO_4$ ($\rho > 1.89$ g ml$^{-1}$) at 100°C for 48 h (ROSENBAUM and SHEPPARD, 1986) in evacuated reaction Y-tubes. For determination of

abundance and isotopic composition of total organic carbon (TOC), powdered samples (250–350 mg) were placed in Vycor tubes (9 × 150 mm) and repeatedly acidified (hot, concentrated HCl) and washed to remove all carbonate. Cupric oxide was mixed with dried, decalcified samples in the same Vycor tubes. These tubes were subsequently evacuated, sealed, and heated at 850°C for 2 h. Recovery and purification of $CO_2$ formed by combustion of organic matter allowed for both quantitative and isotopic analysis.

Oxygen was liberated from chert and magnetite sample powders by reaction with $BrF_5$ in nickel bombs as described by CLAYTON and MAYEDA (1963). Chert and magnetite samples were hand picked under a binocular microscope to remove impurities. Cherts were pretreated with hot, concentrated HCl to remove admixed carbonate; magnetites were not pretreated in this manner. Due to the small sample size, routine magnetic and heavy liquid separation techniques were not employed. As a result, chert and magnetite samples may contain small amounts of iron silicate, iron carbonate, and/or iron oxide. Oxygen was converted to $CO_2$ for isotopic analysis by reaction at a heated graphite electrode.

Carbon dioxide was subsequently isolated by cryogenic distillation and analyzed using a Nuclide, 60°, 6-inch, triple-collector mass spectrometer. Isotopic compositions of $CO_2$ were determined by conventional mass spectrometric techniques (SANTROCK et al., 1985) and are expressed relative to the PDB and SMOW standards: $\delta = 10^3[(R_x/R_{std}) - 1]$, where $R = {}^{13}C/{}^{12}C$ or ${}^{18}O/{}^{16}O$ and the subscript $x$ designates the sample. Fractionation factors employed for calculation of $^{18}O$ abundances of siderite- and ankerite-rich phases based on analyses of $CO_2$ prepared at 100°C were 1.00881 and 1.00901, respectively (ROSENBAUM and SHEPPARD, 1986). Siderite- and ankerite-rich carbonates were generally >80% pure. Fractionation factors were not adjusted to account for effects of minor carbonates present in mixtures.

Elemental compositions of individual coarse-grained carbonates were determined by electron probe microanalysis. Chemical analyses of four oxide components (CaO, MgO, FeO, and MnO) in the carbonates were performed on 12 polished thin sections (1″ diameter) using the 3-spectrometer Etec Autoprobe in the Indiana University Department of Geology. Operating conditions and analytical procedures were as outlined by KLEIN (1974). Each carbonate lamina sampled for isotopic analysis was analyzed an average of three times. Bulk mineralogy of carbonate microbands was determined by staining of thin sections in a solution of alizarin red S and 17 wt% NaOH (HUTCHINSON, 1974), and by X-ray diffraction of whole-rock powders.

Concentrations of major elements in whole-rock powders were determined by inductively coupled plasma atomic emission spectrometry (LECHLER et al., 1980), and the abundance of ferrous iron was determined titrimetrically (modified from SHAPIRO, 1975). Total C and S were quantified using a modified LECO induction furnace with infra-red detectors (model CS-244).

## RESULTS AND DISCUSSION

### Petrography

Microbands are commonly composed of very fine-grained (10–20 μm), granular siderites which form thin, often discontinuous, anastomosing laminae concentrated horizontally in a chert matrix (Fig. 2a). In some cases, these apparently

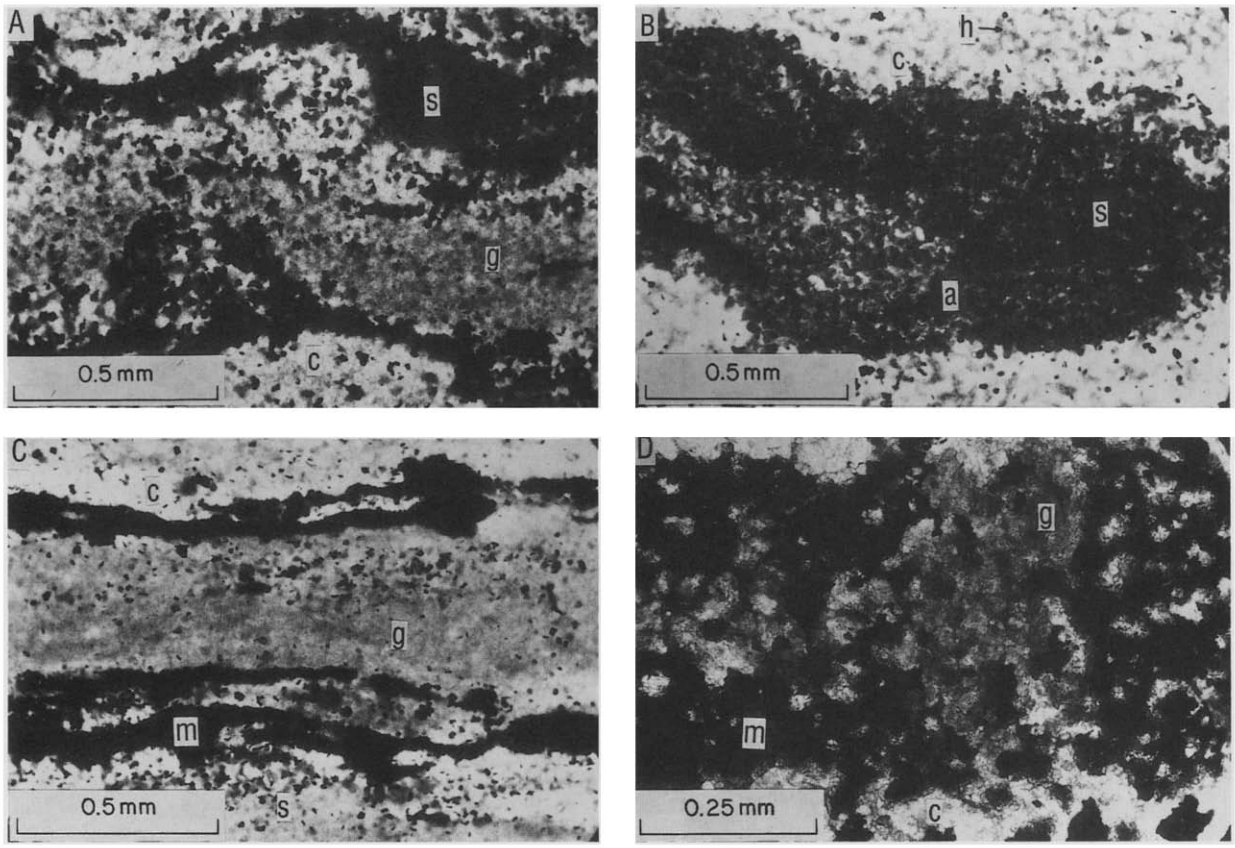


FIG. 2. Photomicrographs of Dales Gorge Member BIF samples: (A) carbonate microbands composed of siderite (s) in a matrix of chert (c) and greenalite (g) (sample P 248); (B) carbonate microbands composed of ankerite (a) and siderite in a matrix of chert and dusty hematite (h) (sample P 255); (C) siderite microbands partially replaced by magnetite (m) (sample P 255); and (D) greenalite microbands partially replaced by magnetite (sample P 248). Siderite grains appear dark due to staining procedure (HUTCHINSON, 1974).

primary siderites are partially replaced by larger (30–50 μm), subhedral ankerites (Fig. 2b), magnetite (Fig. 2c), and/or hematite. Where siderite has been dissolved and replaced by coarse-grained ankerite, the microbands are thicker and less continuous. Ankerites are generally associated with cherts containing very fine-grained hematite, in contrast to siderites, which are predominantly associated with cherts containing amorphous greenalite. Further, ankerites are occasionally replaced by coarse-grained hematite rather than by magnetite. It has been suggested that fine-grained hematite in chert matrix (i.e., jasper) represents a primary precipitate (JAMES, 1954; AYRES, 1972; FRENCH, 1973; DIMROTH and CHAUVEL, 1973; KLEIN and FINK, 1976; EWERS and MORRIS, 1981), but present observations suggest that hematite derives from amorphous greenalite in more oxidized zones. There is no evidence for primary precipitation of magnetite in these samples (cf. KLEIN and BRICKER, 1977). In all cases observed here, both mesobanded and microbanded magnetite derive from either siderite or greenalite (Fig. 2d). Although magnetite and stilpnomelane are minor constituents of the segments from Paraburdoo, they comprise a major fraction of the segment from Wittenoom (Table 1). Magnetite, stilpnomelane, chert, and siderite are intimately intermixed (and typically coarser grained) in the Wittenoom segment. In contrast, essentially monomineralogic laminations are observed in the Paraburdoo segments.

Band-to-band variations in carbonate mineralogy are correlated with variations in the present oxidation state of coexisting minerals. Zones rich in magnetite, greenalite-bearing cherts, and stilpnomelane contain siderite microbands, whereas zones rich in hematite-bearing cherts or cherts lacking fine-grained mineral inclusions contain ankerite microbands. It is likely that these mineralogic variations reflect variations in initial porosity rather than variations in initial oxidation state. The thermodynamically stable assemblage of minerals in unmetamorphosed BIFs indicates highly reducing conditions (KLEIN, 1983) with initial sediments likely composed of colloidal silica and iron hydroxides, amorphous greenalite, and siderite. Whole-rock elemental analyses (Table 1) show that those segments with greater abundances of ankerite (P 234 and P 255) also have higher $Fe^{3+}/Fe^{2+}$ ratios, indicating a greater degree of oxidation. We conclude that oxidizing diagenetic fluids led to the formation of ankerite and hematite at the expense of siderite and greenalite in more permeable regions. In less permeable regions, magnetite was formed at the expense of siderite.

## Isotopic and Chemical Compositions

### *BIF carbonates*

Samples ranging from 3 to 20 mg were collected by microdrilling, split for replicate analysis, and acidified. Depending on the abundance of carbonate in microbands (Table 2), these samples typically yielded at least 5 μmol $CO_2$. Abundances of carbonate minerals in each microband were calculated from measured yields of $CO_2$ assuming the presence of either pure ankerite or siderite. Difficulties were encountered in the electron probe microanalysis of microbanded carbonates. Due to the extremely small size of siderite grains and their intimate mixture with fine-grained chert, quantitative analyses were generally not obtainable. Larger, subhedral carbonates could be analyzed with some accuracy and, in core segments from the Paraburdoo drillhole, were determined to have a composition approximated by $CaMg_{0.6}Fe_{0.4}(CO_3)_2$. In the core segment from the Wittenoom drillhole, coarse-grained carbonates are relatively enriched in iron and have a composition approximated by $CaMg_{0.3}Fe_{0.7}(CO_3)_2$. Chemical compositions of these carbonates most closely approximate those of end member ankerite and are referred to as such in the text. Variations in these "ankerites" are indicated graphically in a ternary Ca-Mg-Fe (Fe + Mn) diagram (Fig. 3).

Results of isotopic analyses of carbonates and sample locations are summarized in Table 2 and illustrated in Figs. 4 and 5. Carbon-isotopic compositions are similar to those previously observed in analyses of BIF carbonate mesobands from the Dales Gorge Member (BECKER and CLAYTON, 1972). The present results (derived mostly from samples from the Paraburdoo core), however, do not reveal a 1.5‰ shift

Table 1. Whole rock analysis of Dales Gorge Member BIF samples

| | Wt % C | | $\delta^{13}C_{org}$ | Wt % | | | | | Wt % | |
|---|---|---|---|---|---|---|---|---|---|---|
| Sample[a] | Carbonate | Organic | (‰ vs. PDB) | Fe | $Fe_2O_3$ | FeO | $Fe^{3+}/Fe^{2+}$ | $SiO_2$ | $Al_2O_3$ | MgO |
| W 97 | 3.59 | 0.067 | -26.20 | 34.4 | 24.0 | 25.22 | 0.86 | 33.0 | 0.28 | 2.70 |
| P 201 | 2.40 | 0.032 | -32.28 | 15.8 | 8.3 | 14.31 | 0.52 | 63.6 | 0.12 | 2.57 |
| P 234 | 2.62 | 0.080 | -32.86 | 26.0 | 27.4 | 9.67 | 2.56 | 47.6 | 0.24 | 2.59 |
| P 248 | 2.89 | 0.082 | -33.29 | 23.5 | 8.9 | 24.74 | 0.32 | 53.2 | 0.24 | 2.62 |
| P 255 | 0.91 | 0.108 | -26.26 | 19.5 | 16.8 | 10.96 | 1.38 | 65.5 | 0.08 | 1.30 |

| | Wt % | | | | | | |
|---|---|---|---|---|---|---|---|
| Sample[a] | CaO | $Na_2O$ | $K_2O$ | MnO | S | Mineralogy[b] | Siderite:Ankerite[c] |
| W 97 | 2.69 | 0.15 | 0.04 | 0.29 | 0.015 | QTZ,SID,MAG,STL,ANK | 73:27 |
| P 201 | 1.90 | 0.03 | 0.10. | 0.12 | 0.039 | QTZ,SID,GRN,ANK,MAG,STL | 83:17 |
| P 234 | 2.37 | 0.03 | 0.14 | 0.13 | 0.024 | QTZ,HEM,SID,MAG,ANK,GRN | 60:40 |
| P 248 | 0.52 | 0.04 | 0.15 | 0.13 | 0.046 | QTZ,SID,GRN,MAG,STL | 100:0 |
| P 255 | 1.49 | 0.03 | 0.12 | 0.05 | 0.018 | QTZ,MAG,HEM,ANK,SID,GRN | 47:52 |

[a]W = Wittenoom; P = Paraburdoo

[b]Determined by X-ray diffraction analysis and listed in descending abundance: QTZ = quartz; HEM = hematite; MAG = magnetite; SID = siderite; ANK = ankerite; GRN = greenalite; STL = stilpnomelane.

[c]Ratio of major peak heights in diffractograms.

Table 2. Isotopic composition of carbonate microbands in the Dales Gorge Member, Brockman Iron Formation, Western Australia[a]

| Vertical distance[b] (mm) | % carbonate[c] (%) | $\delta^{13}C_{PDB}$ (‰) | $\delta^{18}O_{PDB}$ (‰) | $\delta^{18}O_{SMOW}$ (‰) |
|---|---|---|---|---|
| Wittenoom drillhole EC 10, 97 m depth, BIF macroband 13, n = 24 | | | | |
| 0.0 | 43.8 | -10.72 | -10.25 | 20.28 |
| 3.0 | 21.0 | -10.36 | -10.55 | 19.99 |
| 4.5 | 35.4 | -10.63 | -10.01 | 20.54 |
| 6.0 | 30.8 | -10.79 | -10.22 | 20.33 |
| 7.0 | 36.8 | -10.80 | -10.20 | 20.34 |
| 10.0 | 54.5 | -10.92 | -10.26 | 20.27 |
| 27.5 | 9.4 | -10.31 | -10.71 | 19.42 |
| 28.5 | 11.9 | -10.39 | -11.04 | 19.48 |
| 29.5 | 10.4 | -10.47 | -11.14 | 19.38 |
| 31.0 | 18.5 | -10.14 | -11.01 | 19.53 |
| 35.0 | 8.4 | -10.08 | -11.59 | 18.91 |
| 38.0 | 5.5 | -10.38 | -10.36 | 20.18 |
| 39.5 | 16.0 | -10.54 | -10.40 | 20.14 |
| 40.5 | 21.6 | -10.78 | -10.21 | 20.33 |
| 41.0 | 22.9 | -10.77 | -9.59 | 20.97 |
| 42.3 | 22.2 | -10.95 | -10.16 | 20.39 |
| 43.0 | 42.1 | -11.00 | -10.06 | 20.49 |
| 45.5 | 39.8 | -10.85 | -10.48 | 20.06 |
| 49.0 | 57.4 | -9.97 | -11.37 | 19.13 |
| 59.0 | 66.2 | -10.56 | -10.33 | 20.20 |
| 61.0 | 74.4 | -10.52 | -10.37 | 20.16 |
| 66.5 | 62.6 | -9.93 | -9.97 | 20.58 |
| 68.0 | 26.9 | -10.27 | -10.35 | 20.19 |
| 69.0 | 28.1 | -10.39 | -10.65 | 19.88 |
| Paraburdoo drillhole 75-1, 201 m depth, BIF macroband 11, n = 23 | | | | |
| 0.0 | 27.5 | -7.94 | -12.55 | 17.92 |
| 1.2 | 20.8 | -7.96 | -12.53 | 17.95 |
| 2.5 | 20.4 | -7.84 | -12.25 | 18.24 |
| 3.5 | 28.5 | -7.85 | -12.55 | 17.92 |
| 4.0 | 29.2 | -7.95 | -12.61 | 17.92 |
| 5.0 | 27.1 | -7.79 | -12.51 | 17.96 |
| 6.0 | 32.7 | -7.78 | -11.96 | 18.53 |
| 8.0 | 46.0 | -7.96 | -12.05 | 18.43 |
| 9.5 | 36.7 | -7.86 | -11.89 | 18.60 |
| 17.5 | 17.8 | -6.92 | -11.41 | 19.03 |
| 19.0 | 11.5 | -7.21 | -11.14 | 19.37 |
| 20.5 | 14.8 | -7.06 | -11.32 | 19.19 |
| 23.5 | 11.3 | -7.26 | -11.04 | 19.48 |
| 24.5 | 9.9 | -7.00 | -10.71 | 19.82 |
| 30.5 | 11.3 | -7.26 | -11.17 | 19.34 |
| 33.5 | 22.2 | -7.08 | -11.70 | 18.80 |
| 34.5 | 12.3 | -7.32 | -11.74 | 18.76 |
| 36.5 | 16.9 | -7.29 | -11.54 | 18.96 |
| 37.5 | 17.7 | -7.19 | -11.41 | 19.10 |
| 38.5 | 22.3 | -7.54 | -11.53 | 18.97 |
| 39.5 | 18.4 | -7.26 | -11.72 | 18.78 |
| 40.5 | 11.3 | -7.34 | -11.44 | 19.07 |
| 41.5 | 15.4 | -7.38 | -11.88 | 18.61 |
| Paraburdoo drillhole 75-1, 234 m depth, BIF macroband 10, n = 15 | | | | |
| *0.0* | *23.3* | *-7.10* | *-12.70* | *17.78* |
| *2.5* | *18.9* | *-6.83* | *-12.50* | *17.98* |
| *4.0* | *22.5* | *-6.95* | *-12.34* | *18.14* |
| *7.0* | *22.5* | *-6.87* | *-12.03* | *18.47* |
| *8.0* | *24.1* | *-6.95* | *-12.34* | *18.14* |
| *10.0* | *22.8* | *-6.93* | *-12.43* | *18.05* |
| *12.0* | *27.8* | *-7.23* | *-13.19* | *17.27* |
| 31.0 | 47.7 | -7.77 | -12.28 | 18.20 |
| 33.0 | 24.3 | -7.53 | -11.69 | 18.81 |
| 34.0 | 11.4 | -7.64 | -12.23 | 18.25 |
| 35.0 | 10.0 | -7.41 | -11.64 | 18.86 |
| 35.5 | 19.7 | -7.50 | -12.15 | 18.33 |
| 36.5 | 29.8 | -7.47 | -11.93 | 18.56 |
| 37.5 | 11.4 | -7.36 | -12.12 | 18.35 |
| 38.5 | 16.2 | -7.41 | -12.07 | 18.42 |
| Paraburdoo drillhole 75-1, 248 m depth, BIF macroband 10, n = 14 | | | | |
| 0.0 | 26.3 | -8.28 | -12.91 | 17.55 |
| 2.0 | 42.5 | -8.03 | -12.57 | 17.95 |
| 3.0 | 24.6 | -8.18 | -12.12 | 18.37 |
| 5.0 | 14.9 | -8.14 | -12.28 | 18.20 |
| 6.5 | 21.2 | -8.17 | -12.05 | 18.44 |
| 15.5 | 28.0 | -7.98 | -12.55 | 17.92 |
| 17.0 | 42.3 | -8.01 | -12.56 | 17.90 |
| 18.2 | 45.9 | -7.99 | -12.13 | 18.35 |
| 19.0 | 51.3 | -7.93 | -12.05 | 18.43 |
| 20.0 | 44.9 | -7.98 | -12.12 | 18.36 |
| 21.0 | 29.0 | -7.87 | -11.82 | 18.67 |
| 22.0 | 43.3 | -8.08 | -12.35 | 18.12 |
| 23.0 | 38.5 | -8.01 | -12.15 | 18.33 |
| 24.5 | 33.8 | -8.40 | -12.07 | 18.41 |
| Paraburdoo drillhole 75-1, 255 m depth, BIF macroband 9, n = 21 | | | | |
| *0.0* | *15.6* | *-6.73* | *-11.71* | *18.79* |
| *9.0* | *7.4* | *-6.78* | *-11.71* | *18.80* |
| *11.5* | *24.3* | *-6.45* | *-12.03* | *18.47* |
| 21.0 | 5.4 | -7.14 | -11.66 | 18.84 |
| *24.0* | *17.3* | *-6.42* | *-11.31* | *19.20* |
| *26.0* | *9.6* | *-6.49* | *-11.32* | *19.19* |
| 29.0 | 8.1 | -6.43 | -10.96 | 19.58 |
| 30.5 | 7.1 | -7.16 | -11.24 | 19.26 |
| 31.5 | 8.8 | -7.17 | -10.99 | 19.54 |
| 32.5 | 8.3 | -7.13 | -12.06 | 18.42 |
| 34.0 | 4.6 | -7.33 | -11.53 | 18.97 |
| 37.0 | 4.3 | -7.29 | -11.47 | 19.03 |
| 38.0 | 8.8 | -7.17 | -10.99 | 19.54 |
| 39.0 | 8.3 | -7.13 | -12.06 | 18.42 |
| 40.0 | 14.6 | -7.13 | -11.81 | 18.69 |
| 41.0 | 17.1 | -7.32 | -12.22 | 18.26 |
| 42.0 | 8.5 | -7.39 | -12.87 | 17.59 |
| 44.5 | 10.0 | -7.09 | -11.69 | 18.81 |
| 47.0 | 31.2 | -7.08 | -11.75 | 18.75 |
| 48.0 | 78.5 | -7.15 | -12.07 | 18.41 |
| *49.5* | *75.3* | *-7.08* | *-12.19* | *18.29* |

[a]Means of duplicate measurements. 95% confidence intervals are ±0.2%, ±0.19‰, and ±0.35‰ for % carbonate, $\delta^{13}C$, and $\delta^{18}O$ values, respectively. Italicized numbers indicate ankerite-rich microbands.

[b]Vertical distance measurement on polished core segment relative to arbitrary zero point at center of first carbonate microband analyzed in each segment.

[c]Wt. % carbonate mineral, calculated from micromoles $CO_2$ per mg rock powder, assuming all carbonate is siderite $FeCO_3$ or ankerite $Ca_2MgFe(CO_3)_4$.

n.d. = none detected

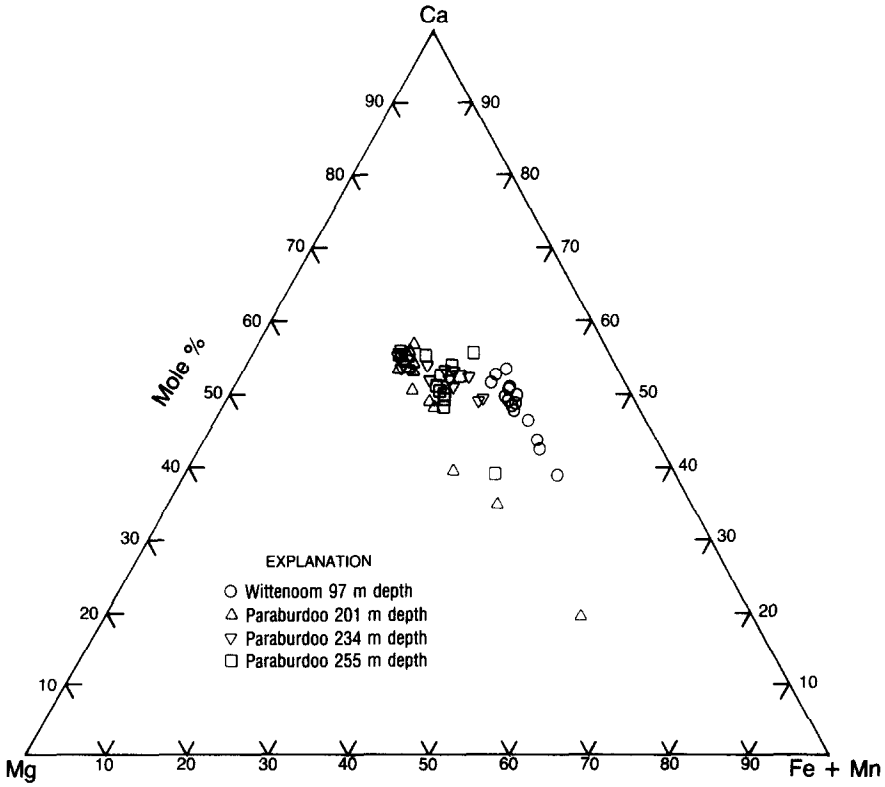


FIG. 3. Range of elemental compositions of coarse-grained carbonates in core segments from depths of 201, 234, and 255 m in Paraburdoo drillhole 75-1, and in a core segment from a depth of 97 m in Wittenoom drillhole EC-10. Each point represents the average of three analyses for each microband. Averaged carbonate compositions which fall below the ferroan dolomite-ankerite series (i.e., below 45 mol% Ca) are the result of coexisting carbonates not resolved by the electron microprobe beam during the tranverse across an individual lamina and, therefore, represent a two-phase assemblage.

to more negative $\delta^{13}C$ values between BIF macrobands 10 and 11. BECKER and CLAYTON (1972) observed this shift in samples from the Wittenoom core, and the isotopic compositions observed here for samples from BIF macroband 13 in the Wittenoom core indicate that the shift extends upward at Wittenoom to at least that level. Whatever change led to the 1.5‰ shift at Wittenoom, it must have resulted from factors that were inoperative or neutralized at Paraburdoo. Oxygen-isotopic compositions of microbanded carbonates from Paraburdoo are depleted by 0.5 to 2.0‰ relative to microbanded and mesobanded carbonates from Wittenoom. Carbonate microbands from Wittenoom are also more strongly depleted in $^{13}C$($\delta^{13}C \sim -10.5$‰) relative to those from Paraburdoo ($\delta^{13}C \sim -7$‰, see Fig. 5), a feature roughly correlated with the abundance of iron in whole-rock samples (Table 1).

Isotopic contrasts between successive microbands are typically small; most band-to-band variations are less than 0.5‰ for both $^{13}C$ and $^{18}O$ (see Fig. 4). Similar small variations are noted in carbonate microbands from the Kuruman Iron Formation, South Africa (KAUFMAN, unpubl. results). These observations are in marked contrast to wide variations in the isotopic composition of BIF microbands reported from the Marra Mamba Iron Formation and Bruno's Band of the Mount Sylvia Formation (BAUR et al., 1985). Review of analytical procedures used by BAUR et al. (1985) indicates that most of their samples yielded less than 1.0 $\mu$mol $CO_2$. Laboratory records show that difficulties were encountered in the mass spectrometric analysis of many of the extremely small gas samples. Most of the extremely depleted isotopic compositions reported are associated with very small $CO_2$ samples, with abbreviated mass spectrometric analyses, or with samples for which replicate analyses were not obtained. Accordingly, conclusions of BAUR et al. (1985) will bear reexamination here.

### *BIF cherts and magnetites*

Results of oxygen-isotopic analyses of cherts and magnetites together with their sample locations are listed in Table 3 and illustrated in Fig. 4. Isotopic compositions of chert and magnetite in microbands from Paraburdoo fall in the same range as those of chert and magnetite in mesobands from Wittenoom (BECKER and CLAYTON, 1976). The presence of abundant siderite in the magnetite sample from 48 mm depth in the P 255 core segment may account for its enriched oxygen-isotopic composition relative to other magnetite samples lacking admixed siderite (Table 3). Fractionation of oxygen isotopes between chert and coexisting magnetite or iron-bearing carbonate has been used to estimate temperatures of final equilibration in many Precambrian BIFs (see reviews by PERRY, 1983; MÜLLER et al., 1986). In mesoband samples

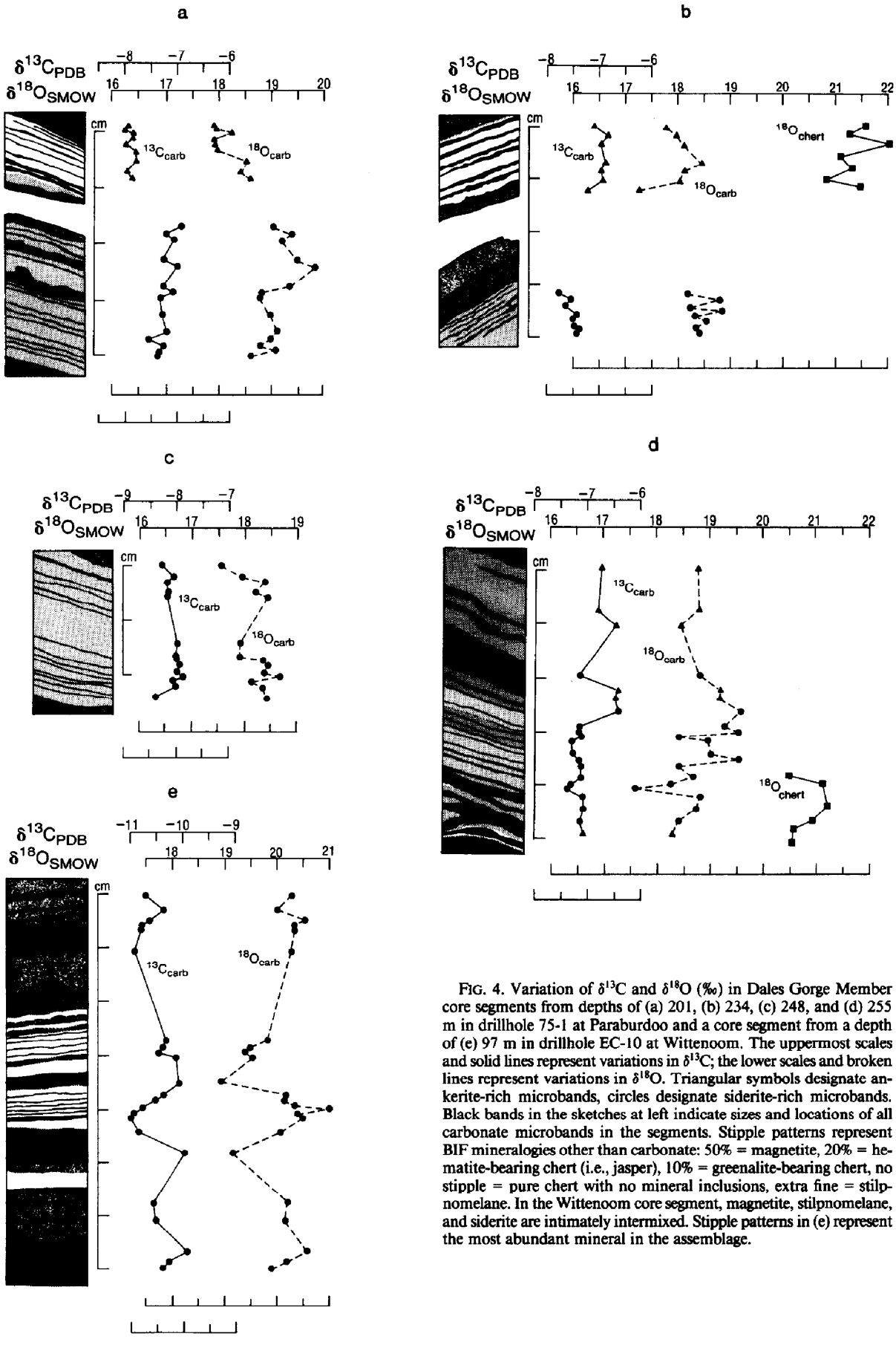


FIG. 4. Variation of $\delta^{13}C$ and $\delta^{18}O$ (‰) in Dales Gorge Member core segments from depths of (a) 201, (b) 234, (c) 248, and (d) 255 m in drillhole 75-1 at Paraburdoo and a core segment from a depth of (e) 97 m in drillhole EC-10 at Wittenoom. The uppermost scales and solid lines represent variations in $\delta^{13}C$; the lower scales and broken lines represent variations in $\delta^{18}O$. Triangular symbols designate ankerite-rich microbands, circles designate siderite-rich microbands. Black bands in the sketches at left indicate sizes and locations of all carbonate microbands in the segments. Stipple patterns represent BIF mineralogies other than carbonate: 50% = magnetite, 20% = hematite-bearing chert (i.e., jasper), 10% = greenalite-bearing chert, no stipple = pure chert with no mineral inclusions, extra fine = stilpnomelane. In the Wittenoom core segment, magnetite, stilpnomelane, and siderite are intimately intermixed. Stipple patterns in (e) represent the most abundant mineral in the assemblage.

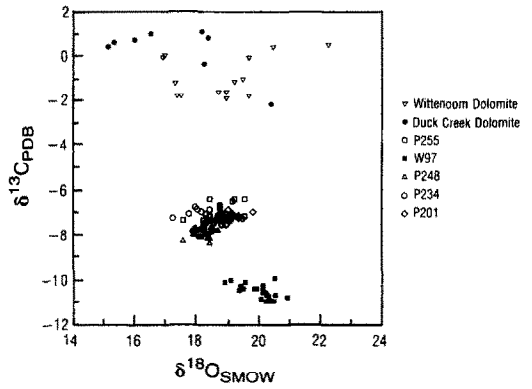


FIG. 5. Crossplot of $\delta^{13}C$ and $\delta^{18}O$ in microbanded carbonates in core segments from depths of 201, 234, 248, and 255 m in drillhole 75-1 at Paraburdoo and from a depth of 97 m in drillhole EC-10 at Wittenoom. The ranges of carbon and oxygen isotope variations determined from samples of the Wittenoom and Duck Creek dolomites are also indicated.

from Wittenoom, isotopic differences between coexisting chert and siderite are small. Δ(QTZ-SID) ranges from −0.04 to +1.08‰, indicating temperatures ranging from 270 to 370°C (BECKER and CLAYTON, 1976). In comparison, isotopic differences between adjacent laminations of chert and siderite (or ankerite) in core segments from Paraburdoo are larger and more variable (Table 3). Some variability in $^{18}O$ abundances of chert microbands may result from analytical uncertainty and/or from admixture of traces of iron silicate or iron oxide minerals. However, because addition of oxygen from impurities in chert samples would tend to decrease rather than increase observed isotopic differences, this could not be the cause of larger isotopic fractionations observed in samples from Paraburdoo (relative to those from Wittenoom). If Δ(QTZ-SID) values observed in this study are plotted on Fig. 4 of BECKER and CLAYTON (1976), they yield temperatures of final equilibration ranging from approximately 60 to 160°C and averaging approximately 100°C. The ubiquitous presence of greenalite in core segments from Paraburdoo (Table 1) similarly suggests that temperatures never exceeded 150°C (FRENCH, 1973; KLEIN and FINK, 1976; KLEIN, 1983; MIYANO and BEUKES, 1984; MIYANO, 1987). These observations are consistent with the findings of EWERS and MORRIS (1981) indicating increasing metamorphic grade from Paraburdoo to Wittenoom.

Correlated variations in $\delta^{18}O$ values led BECKER and CLAYTON (1976) to conclude that chert and carbonate at Wittenoom were in "almost complete isotopic equilibrium with one another through an interstitial fluid whose isotopic composition was essentially controlled by quartz." Furthermore, they indicate that equilibration occurred over distances on the scale of centimeters. Millimeter-scale variability in $\delta^{18}O$ of chert and in Δ(QTZ-SID) or Δ(QTZ-ANK) at Paraburdoo suggests

1) disequilibrium conditions,
2) oxygen-isotopic exchange with other BIF minerals,

Table 3. Oxygen isotope abundances of chert and magnetite microbands[a]

| segment | sample | Vertical distance[b] | mineralogy[c] | $\delta^{18}O_{SMOW}$ (‰) | ΔQTZ-ANK or QTZ-SID[d] (‰) | ΔQTZ-MAG[e] (‰) |
|---|---|---|---|---|---|---|
| P 234 | M1 | -2.0 | MAG (SID,QTZ) | -0.91 | | |
| | C2 | -1.0 | QTZ (GRN) | 21.51 | 3.46 | 22.42 |
| | C3 | 1.5 | QTZ (GRN) | 20.83 | 2.69-2.78 | |
| | C4 | 3.2 | QTZ (GRN) | 21.33 | 2.86-3.19 | |
| | C5 | 5.5 | QTZ (GRN) | 21.11 | 2.64-2.97 | |
| | C6 | 7.5 | QTZ (GRN) | 22.04 | 3.90-4.06 | |
| | C7 | 9.0 | QTZ (GRN) | 21.27 | 3.29-3.49 | |
| | C8 | 11.0 | QTZ (GRN) | 21.59 | 3.81 | |
| P 255 | C(B)7 | 40.5 | QTZ (GRN,MAG) | 20.48 | 1.79-2.22 | |
| | C(B)6 | 41.5 | QTZ (GRN,MAG) | 21.14 | 2.88-3.55 | |
| | M(B)2 | 43.0 | MAG (SID,QTZ) | 1.18 | | |
| | C(B)5 | 44.0 | QTZ (GRN) | 21.74 | 2.41 | 20.56 |
| | C(B)3 | 46.0 | QTZ (GRN) | 21.22 | 2.93-2.99 | |
| | C(B)4 | 48.0 | QTZ (GRN) | 20.91 | 2.50 | 12.35 |
| | M(B)1 | 48.0 | MAG (SID) | 8.56 | | |
| | C(B)2 | 49.0 | QTZ (GRN) | 20.55 | 2.33 | 11.99 |
| | C(B)1 | 50.5 | QTZ (GRN) | 20.59 | 2.26 | |

[a]Averages of replicate analyses. 95% confidence interval = ±0.32‰.

[b]Vertical distance as measured in mm from the center of the first carbonate microband in the segment (see Table 2).

[c]QTZ = quartz, MAG = magnetite, SID = siderite, GRN = greenalite. Parentheses designate minor components.

[d]Isotopic difference between chert microband and neighboring carbonate microband.

[e]Isotopic difference between chert microband and neighboring magnetite microband.

3) admixture of iron silicates and/or iron oxides to chert samples.

If the variability in $^{18}O$ abundances of chert microbands is a function of either 1) or 2), it would convincingly argue against the open-system characteristics suggested for the Hamersley BIFs (GREGORY, 1986; GREGORY and CRISS, 1986) wherein large volumes of oxygen (from an external source, likely surface waters) led to homogenization of isotopic compositions. Possible causes of isotopic variations in BIF microbands will, therefore, be investigated.

### Causes of Isotopic Variations Between Microbands

Band-to-band variations in abundances of $^{13}C$ and $^{18}O$ in carbonates are, on average, 0.2 and 0.3‰, respectively. The statistical significance of these variations is marginal, but 35% of the $^{13}C$ shifts and 42% of the $^{18}O$ shifts exceed the 95% confidence limit for duplicate analyses (Table 2). Figure 4 indicates that these relatively abrupt shifts accompany mineralogic changes (siderite → ankerite or siderite → magnetite). Petrographic and elemental analyses (Table 1) suggest that zones where ankerites formed were more open to oxidizing diagenetic fluids. Accordingly, the marginally significant band-to-band variations are probably associated with minor differences in isotopic compositions of diagenetic fluids.

Alternatively, isotopic variations between carbonate microbands with different chemical compositions might be a function of mineral-dependent fractionations. For example, the equilibrium oxygen-isotopic fractionations expected between ankerites analyzed here (Fig. 3) can be approximated using the relationship empirically derived by ROSENBAUM and SHEPPARD (1986) for carbonates in the $CaCO_3$ – (Ca, Mg)$CO_3$ – $FeCO_3$ system at 100°C:

$$1000\ln\alpha = 8.94X_{CaCO3} + 9.29X_{MgCO3} + 8.77X_{FeCO3},$$

where $X_i$ represents the mole fraction of component i in the carbonate. Based on this relationship, maximal differences expected among $^{18}O$ abundances in ankerites from both Paraburdoo and Wittenoom are less that 0.1‰. Oxygen-isotopic differences expected among siderites cannot be calculated because microprobe analyses could not be obtained from these fine-grained carbonates. Differences among siderites are, however, expected to be smaller than those among ankerites. Although no experimental data exist on the fractionation of isotopes of carbon and oxygen between coexisting carbonate pairs other than dolomite and calcite, theoretical calculations (GOLYSHEV et al., 1981) are in agreement with experimental results for that mineral pair. The same calculations can be extended to estimate equilibrium fractionations of carbon and oxygen isotopes associated with chemical variations in the BIF carbonates. Figure 6 shows fractionations of carbon and oxygen isotopes calculated from data presented by GOLYSHEV et al. (1981) for carbonate pairs at temperatures ranging from 0 to 1000°C. Also indicated are the isotopic fractionations and metamorphic equilibration temperatures of natural samples used by SHEPPARD and SCHWARCZ (1970) in their derivation of expressions for the fractionation of carbon and oxygen isotopes between coexisting dolomite and calcite. To apply these fractionations to BIF carbonates, metamorphic equilibration temperatures must be determined.

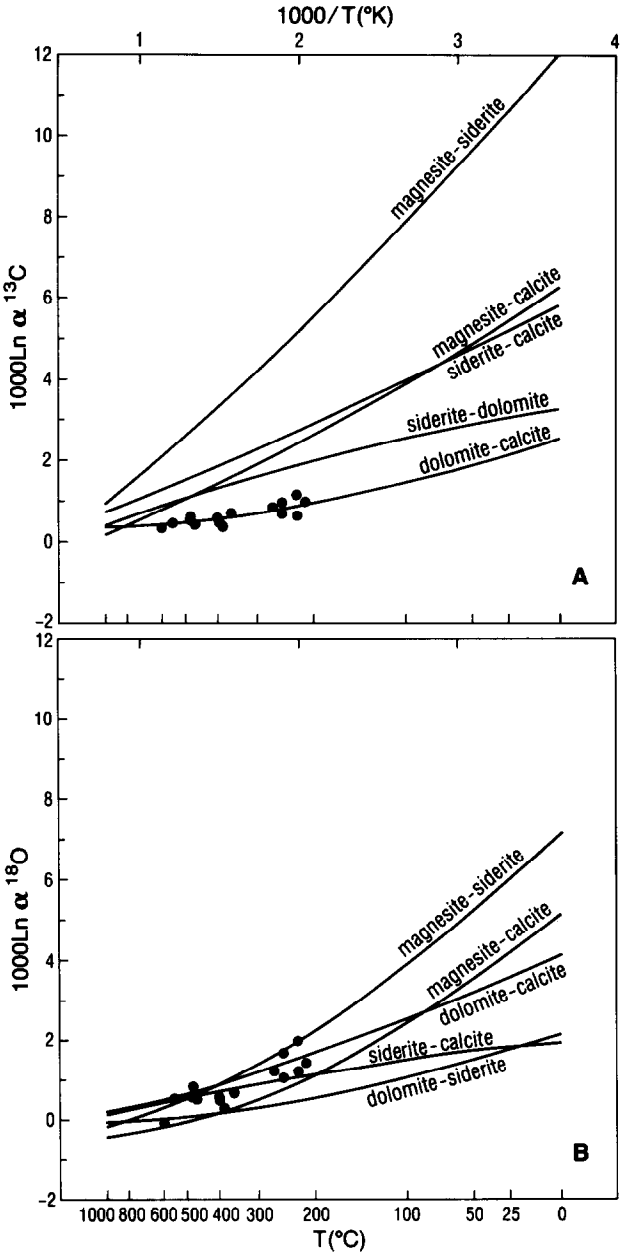


FIG. 6. Predicted mineral-dependent fractionations [(A) 1000 ln $\alpha^{13}C$; (B) 1000 ln $\alpha^{18}O$] for coexisting endmember carbonate compositions at temperatures ranging from 0 to 1000°C (calculated from GOLYSHEV et al., 1981). The first mineral in each pair is enriched in the heavy isotope relative to the second mineral. Points represent the isotopic fractionations and metamorphic equilibration temperatures of natural samples used by SHEPPARD and SCHWARCZ (1970) to derive expressions for the fractionation of carbon and oxygen between coexisting dolomite and calcite.

For the Paraburdoo strata studied here, Δ(QTZ-SID) values (Table 3) indicate temperatures of approximately 100°C. Referring to Fig. 6, isotopic differences expected between siderite and dolomite at 100°C are approximately 0.8‰ for O and 2.0‰ for C (the empirical relationship noted above indicates isotopic differences of 0.35‰ for O at 100°C). How-

ever, siderite would be enriched in $^{13}C$ and depleted in $^{18}O$ relative to dolomite. In many of these samples, the opposite relationship is observed. If any single pair of isotopic measurements is considered in isolation, the small differences appear hardly worthy of consideration. But the pattern of isotopic variations, petrographic textures, and mineralogic compositions can, overall, be most simply and consistently interpreted as diagenetic in origin, with variations in isotopic composition being due to variations in the composition of diagenetic fluids.

Oxygen-isotopic exchange among carbonates, cherts, and other BIF minerals during diagenetic or metamorphic alteration may be responsible for variation of $^{18}O$ abundances observed in this study. The most distinct band-to-band variations in oxygen-isotope compositions in the Paraburdoo core segments are found in siderite microbands that are partially altered to magnetite; siderite microbands that show no textural evidence of alteration yield relatively constant $\delta^{18}O$ values. For example, in core segment P 255 (Fig. 4d), significant band-to-band variations in $^{18}O$ abundances are associated with siderite microbands partially altered to magnetite (samples from 31.5 to 42.0 mm in Table 2; see also Fig. 2c). In core segment P 201 (Fig. 4a), siderite microbands isolated from a horizon where lenticular magnetite crystals have formed (samples from 17.5 to 33.5 mm in Table 2) similarly exhibit the largest variations in oxygen-isotopic compositions within the segment. Magnetite in BIF is typically depleted in $^{18}O$ relative to both chert and carbonate (Table 3; see also the results of BECKER and CLAYTON, 1976). It appears that the isotopic compositions of residual carbonates were influenced by fluids mediating the formation of magnetite in these zones.

Regardless of whether the variation in $^{18}O$ is caused by the diagenetic replacement of siderite by ankerite or by magnetite, millimeter-scale variations in BIF carbonates must have been controlled by processes working on a fine scale and were apparently not affected by large volumes of fluids with isotopic compositions controlled by an external reservoir (cf. GREGORY, 1986; GREGORY and CRISS, 1986).

### Causes of Overall Depletion of $^{13}C$

It has often been suggested that overall depletion of $^{13}C$ in BIF carbonates reflects the presence of carbonate derived from oxidation of organic carbon. This process was first suggested explicitly by PERRY et al. (1973), who concluded that "diagenesis or metamorphism" might drive the reaction. With few exceptions (WALKER, 1984; BAUR et al., 1985), most subsequent authors have considered the oxidation of organic C at the expense of $Fe^{3+}$ in terms of thermally-driven reactions. In the Dales Gorge Member, higher concentrations of iron at Wittenoom are correlated with greater degrees of $^{13}C$ depletion, a correlation also observed in samples from the Kuruman Iron Formation, South Africa (BEUKES et al., 1990; see also PERRY et al., 1973). Independent of any possible association with sedimentary redox reactions, the correlation between $^{13}C$ depletion and iron abundance has been noted in numerous localities.

Recent elemental and isotopic studies of a transition from stromatolitic carbonates to BIF in the Transvaal Supergroup, South Africa, suggest that early Proterozoic oceans were stratified, with a lower water mass depleted in $^{13}C$ (BEUKES et al., 1990). Abundance patterns of rare earth elements (REEs) in the BIF sediments suggest a hydrothermal source for Fe (KLEIN and BEUKES, 1989). Upwelling apparently brought deep, anoxic waters to shelves where siderites with isotopic compositions near −5‰ formed below the chemocline, while limestones with isotopic compositions near −1‰ formed in shallow, near-shore environments that iron in upwelling waters could not reach because of the presence of $O_2$ (BEUKES et al., 1990). According to this view, a portion of the carbon-isotopic depletion observed in BIF carbonates (i.e., the difference between the limestones and the primary siderites) derives from depletion of $^{13}C$ in dissolved inorganic carbon in a lower portion of the water column. The additional depletion (i.e., that required to produce carbonates with $\delta < -5‰$), which we will term secondary, derives from postdepositional processes. Noting that carbonates in oxide-rich BIF are depleted in $^{13}C$ relative to those in siderite-rich BIF, BEUKES et al. (1990) suggest that organic carbon "was removed in the oxide facies by oxidation at the expense of $Fe^{3+}$ (as part of inorganic reactions during diagenesis)," and that this "contributed to the depletion of $^{13}C$ in the carbonates" in the oxide facies.

If a similar interpretation were applied to the Dales Gorge Member, isotopic compositions of the samples from Paraburdoo ("siderite-rich BIF" in the classification of BEUKES et al., 1990) would be viewed as recording mainly the depletion of $^{13}C$ in water-column carbonate. However, because these samples contain significant quantities of magnetite, exhibit variable $^{13}C$ contents (−6.4 to −8.4‰), and are more strongly depleted in $^{13}C$ than the Kuruman siderite microsparites, it is likely that at least some of the isotopic depletion derives from diagenetic processes. We follow BEUKES et al. (1990) in suggesting an initial $\delta$ value of −5‰ and, thus, estimate secondary shifts ranging from 1 to 3‰. Samples from Wittenoom contain significantly more iron and are comparable to the "magnetite-rich BIF" facies identified by BEUKES et al. (1990). Carbonates from these samples have $-9.9 \geq \delta \geq -11.0$ and may, thus, reflect secondary shifts of 5 to 6‰.

Concentrations of organic carbon are low in all of the samples examined here. The presence of primary siderite indicates sedimentary redox conditions that would have favored preservation of organic carbon (the near absence of sulfur excludes sulfate reduction; nitrate reduction remains a possibility, but there is no evidence that it was a significant biogeochemical process at this time). It follows either that (1) only traces of organic carbon fell from the water column into the accumulating sediment or (2) amounts of coprecipitated $Fe^{3+}$ were always more than adequate for complete oxidation of organic carbon falling into the sediment. The second possibility is complex. It is, for example, possible that inputs of iron and organic matter covaried, since the same factors (e.g., upwelling) that increased production and sedimentation of organic matter might also have stimulated precipitation of iron oxide. The larger secondary isotopic shifts at Wittenoom can be correlated with the significantly larger concentrations of iron. In 100 g of Wittenoom material, there are 620 mmol Fe and 300 mmol carbonate C. If the latter derives from a

mixture of primary carbonate with $\delta = -5‰$ and secondary carbonate with $\delta = -35‰$ (estimated from the isotopic composition of organic material in organic-carbon-rich Hamersley sediments, HAYES et al., 1983), then 55 mmol carbonate C derive from oxidation of organic carbon. Because each mmol of organic carbon requires four mmol of ferric iron for oxidation, the mechanism suggested by BEUKES et al. (1990) would require that coprecipitated $Fe^{3+}$ amounted to at least 220 mmol. Indeed, this is roughly the difference between sediments at Paraburdoo (average 380 mmol Fe per 100 g rock) and Wittenoom. The correlation would be far more impressive if redox levels of iron could be taken into account and the depletion of $^{13}C$ in carbonate correlated with the reduction of $Fe^{3+}$, but the petrographic observations summarized above indicate clearly that redox levels of Fe have been altered by diagenetic processes. Moreover, at Paraburdoo, carbon-isotopic depletion is not well correlated with iron abundance. If, however, the stratified-ocean model and its associated control of isotopic abundances were abandoned in favor of a system in which all of the isotopic depletion (i.e., from seawater with $\delta \sim -1‰$ to carbonate minerals with $\delta \sim -7$ or $-10.5‰$) were ascribed to *in situ* oxidation of organic carbon, (1) the correlation between $^{13}C$ depletion and abundance of iron oxide would not be explained, and (2) isotopic compositions in the range between $-1$ and $-5‰$, not observed in any unmetamorphosed iron-formation, would be expected.

A metamorphic (post-lithification) origin for the secondary ($\delta < -5‰$) carbon-isotopic depletion is unlikely. In the case of the Wittenoom samples, for example, it would be required that the rock initially contained at least 0.7% organic carbon, that the subsequent oxidation of this carbon was absolutely quantitative, and that the $CO_2$ was somehow retained as carbonate as other oxidation products escaped. BAUR et al. (1985) noted that preservation of large isotopic variations between microbands is inconsistent with a metamorphic origin for $^{13}C$-depleted carbonate. This conclusion was based on the assumed presence of a fluid phase, as well as on the inevitable mobility of the reaction product ($CO_2$). Results of analyses presented here indicate that extreme carbon-isotopic variations are not characteristic features of carbonate BIF microbands. However, band-to-band variations up to 0.9‰ are evident in samples from Paraburdoo which were not heated to temperatures above 160°C and in which textural and mineralogic evidence of metamorphism is lacking. On balance, we conclude that the secondary depletion of and millimeter-scale variation in the abundance of carbon-13 is better attributed to a low temperature process. The transfer of electrons from organic carbon to ferric iron at low temperature (i.e., oxidation of organic matter and reduction of $Fe^{3+}$) is an exergonic process commonly exploited by bacteria as a source of energy (GHIORSE, 1988). Accordingly, we concur with BECKER and CLAYTON (1972), WALKER, (1984), and BAUR et al. (1985) in suggesting that carbonate derived from organic matter was biologically produced within these sediments prior to lithification.

### Comparison to Wittenoom and Duck Creek Dolomites

Isotopic compositions of microbanded BIF carbonates can be compared with those of whole-rock samples from the Wittenoom and Duck Creek Dolomites (see Fig. 5). The Wittenoom Dolomite lies approximately 150 m below the Dales Gorge Member in the Hamersley Group. It is composed of very uniform, massive, medium- to thinly bedded dolomite containing up to 1.1 wt% MnO (0.95 ± 0.13 wt%, mean ± s. d., n = 14) with thin bands of intercalated carbonaceous shales containing up to 11.9 wt% $K_2O$ (8.7 ± 1.6 wt%, n = 17; DAVY, 1975). The concentration of FeO in samples from the Wittenoom Dolomite is low (2.89 wt%, mean, n = 14; DAVY, 1975) compared to whole-rock BIF samples from Paraburdoo and Wittenoom (Table 1). The Duck Creek Dolomite of the Wyloo Group, in the Hamersley Basin, is composed of stromatolitic and clastic-textured dolomites and has been interpreted as a repeating sequence of upward-shallowing sabkha-type deposits (THORNE, 1983). No elemental or petrographic analyses of the Duck Creek Dolomite are presently available. The range of oxygen-isotopic compositions of BIF microbanded carbonates is smaller than the range of reported values of massive Wittenoom and Duck Creek dolomites (BECKER and CLAYTON, 1976; SCHIDLOWSKI et al., 1983). The origin of such large oxygen-isotopic variations in massive Precambrian carbonates is unclear, but it seems possible that these carbonates were more permeable to diagenetic fluids (likely leading to dolomitization) than the siliceous iron formations. Carbon-isotopic compositions of the massive carbonates suggest deposition from the upper layer of the early Proterozoic ocean probably in shallow, oxygenated water (KLEIN and BEUKES, 1989; BEUKES et al., 1990).

Oxygen-isotopic compositions of the BIF carbonates and of under- and overlying marine dolostones (i.e., the Wittenoom and Duck Creek dolomites) fit into secular trends previously determined for carbonates formed in the late Archean/early Proterozoic ocean (VEIZER, 1983). Other chemical evidence for the marine origin of the Hamersley BIFs includes the isotopic abundances of neodymium (JACOBSEN and PIMENTEL-KLOSE, 1988) and sulfur (CAMERON, 1982) and abundances of REEs and other trace elements (DAVY et al., 1977; GRAF, 1977; FRYER, 1979, 1983; KLEIN and BEUKES, 1989). The conspicuous absence of clastic materials in the Dales Gorge Member further substantiates a marine origin for the BIF.

## CONCLUSIONS

Patterns of variation in isotopic abundance and mineral composition can be consistently explained in terms of diagenetic replacement of fine-grained primary precipitates. The extent of diagenetic replacement appears to have been controlled by variations in the permeability of sediments. In more permeable, oxidized zones, primary siderite and greenalite were replaced by ankerite and hematite, while in less permeable zones with intermediate levels of oxidation, siderites were commonly replaced by magnetite. The general depletion of $^{13}C$ in microbanded and mesobanded carbonates is attributed to their formation in an isotopically depleted water mass enriched in Fe and depleted in $^{13}C$. The most likely sources for this water are hydrothermal vents in the deep ocean. Although high-temperature oxidation of organic carbon could have led to carbonates depleted in $^{13}C$, it is unlikely that lithified rocks contained enough organic matter to sustain

the reaction to subsequently produce carbonates with $\delta^{13}C$ near −10‰. Further, the preservation of mm-scale variations of $^{13}C$ and $^{18}O$ in laminations of carbonate and chert from both metamorphosed and unmetamorphosed BIF is inconsistent with a metamorphic origin for much additional depletion of $^{13}C$. On the other hand, some degree of additional $^{13}C$ depletion likely results from biological oxidation of organic carbon in unlithified sediments linked to initial abundances of Fe and organic carbon.

Variations in the magnitude of oxygen-isotopic fractionations between chert and carbonate and in mineral assemblages in samples from Paraburdoo and Wittenoom record effects of prograde metamorphism across the Hamersley Basin. At Paraburdoo, near the southern border of the basin, oxygen-isotopic fractionations suggest temperatures of burial metamorphism near 100°C, consistent with the ubiquitous presence of greenalite in these samples. Smaller oxygen-isotopic differences in samples from Wittenoom, near the northern border of the basin, suggest metamorphic temperatures near 300°C (BECKER and CLAYTON, 1976), consistent with the presence of minnesotaite in nearby samples (MIYANO, 1987). These observations highlight the need for detailed intrabasinal studies of early Proterozoic sedimentary basins.

*Acknowledgments*—Materials for this study were made available to C.K. and J.M.H. through the generous cooperation of R. C. Morris, CSIRO, Wembley, WA, Australia. Oxygen-isotopic compositions of samples of chert and magnetite were measured in the laboratories of Professor S. M. Savin, Case Western Reserve University. We greatly appreciate Professor Savin's generous cooperation and advice. We thank S. A. Studley for assistance with isotopic analyses and laboratory procedures, and H. D. Holland, J. A. McKenzie, T. F. Anderson, E. M. Ripley, E. Merino, and R. P. Wintsch for their valuable comments on and criticisms of this work. We thank R. Y. Anderson, C. J. Yapp, Z. Sharp, R. H. Becker, F. J. Longstaffe, and, especially, E. C. Perry for constructive reviews of earlier versions of this paper. This work was supported by NASA grant NGR 15-003-118 to J.M.H. and NSF grants EAR 82-05473 and 84-19161 to C.K.

*Editorial handling:* B. E. Taylor

## REFERENCES

AYRES D. E. (1972) Genesis of iron-bearing minerals in banded iron-formation mesobands in the Dales Gorge Member, Hamersley Group, Western Australia. *Econ. Geol.* **67,** 1214–1233.

BAUR M. E., HAYES J. M., STUDLEY S. A., and WALTER M. R. (1985) Millimeter-scale variations of stable isotope abundances in carbonates from banded iron-formations in the Hamersley Group of Western Australia. *Econ. Geol.* **80,** 270–282.

BECKER R. H. and CLAYTON R. N. (1972) Carbon isotopic evidence for the origin of banded iron-formation in Western Australia. *Geochim. Cosmochim. Acta* **36,** 577–595.

BECKER R. H. and CLAYTON R. N. (1976) Oxygen isotope study of a Precambrian banded iron-formation, Hamersley Range, Western Australia. *Geochim. Cosmochim. Acta* **40,** 1153–1165.

BEUKES N. J., KLEIN C., KAUFMAN A. J., and HAYES J. M. (1990) Carbonate petrography, kerogen distribution and carbon and oxygen isotope variations in an Early Proterozoic transition from limestone to iron-formation deposition, Transvaal Supergroup, South Africa. *Econ. Geol.*, **85,** 663–690.

CAMERON E. M. (1982) Sulfate and sulfate reduction in early Precambrian oceans. *Nature* **296,** 145–147.

CLAYTON R. N. and MAYEDA T. K. (1963) The use of bromine pentafluoride in the extraction of oxygen from oxides and silicates for isotopic analysis. *Geochim. Cosmochim. Acta* **27,** 43–52.

DAVY R. (1975) A geochemical study of a dolomite-BIF transition in the lower part of the Hamersley Group. *Geol. Surv. W. Australia Annual Rept., 1974,* pp. 88–100.

DAVY R., BRAKEL A. T., and MUHLING P. C. (1977) The value of B-Ga-Rb diagrams in determining depositional conditions in Proterozoic rocks in the northwest of Western Australia. *Geol. Surv. W. Australia Annual Rept. 1976,* pp. 80–85.

DIMROTH E. (1968) Sedimentary textures, diagenesis, and sedimentary environment of certain Precambrian ironstones. *N. Jahrb. Geol. Palaontol.* **130,** 247–274.

DIMROTH E. and CHAUVEL J. J. (1973) Petrography of the Sokoman Iron Formation in part of the central Labrador Trough, Quebec, Canada. *Geol. Soc. Amer. Bull.* **84,** 111–134.

EWERS W. E. (1980) Chemical conditions for the precipitation of banded iron-formations. In *Biochemistry of Ancient and Modern Environments* (eds. P. A. TRUDINGER et al.), pp. 83–92. Australian Academy of Science.

EWERS W. E. (1983) Chemical factors in the deposition and diagenesis of banded iron-formation. In *Iron-Formation: Facts and Problems* (eds. A. F. TRENDALL and R. C. MORRIS), pp. 491–510. Elsevier.

EWERS W. E. and MORRIS R. C. (1981) Studies of the Dales Gorge Member of the Brockman Iron Formation, Western Australia. *Econ. Geol.* **76,** 1929–1953.

FRENCH B. M. (1973) Mineral assemblages in diagenetic and low-grade metamorphic iron-formation. *Econ. Geol.* **68,** 1063–1075.

FRYER B. J. (1979) Rare earth evidence in iron-formations for changing Precambrian oxidation states. *Geochim. Cosmochim. Acta* **41,** 361–367.

FRYER B. J. (1983) Part B: Rare earth elements in iron-formation. In *Iron-Formation: Facts and Problems* (eds. A. F. TRENDALL and R. C. MORRIS), pp. 345–357. Elsevier.

GARRELS R. M. (1987) A model for the deposition of the microbanded Precambrian iron formations. *Amer. J. Sci.* **287,** 81–106.

GHIORSE W. C. (1988) Microbial reduction of manganese and iron. In *Biology of Anaerobic Microorganisms* (ed. A. J. B. ZEHNDER), pp 305–332. J. Wiley & Sons.

GOLYSHEV S. I., PADALKO N. L., and PECHENKIN S. A. (1981) Fractionation of stable oxygen and carbon isotopes in carbonate systems. *Geokhimiya* **10,** 1427–1441.

GRAF J. L., JR. (1977) Rare earth elements, iron formations and sea water. *Geochim. Cosmochim. Acta* **42,** 1845–1850.

GREGORY R. T. (1986) Oxygen isotope systematics of quartz-magnetite pairs from Precambrian iron-formations: Evidence for fluid-rock interactions during diagenesis and metamorphism. In *Fluid Rock Interactions during Metamorphism* (eds. J. V. WALTHER and B. J. WOOD), pp. 132–153. Springer-Verlag.

GREGORY R. T. and CRISS R. E. (1986) Isotopic exchange in open and closed systems. In *Stable Isotopes in High Temperature Geological Processes* (eds. J. W. VALLEY et al.); *Reviews in Mineralogy 16,* pp. 91–127.

HAYES J. M., KAPLAN I. R., and WEDEKING K. W. (1983) Precambrian organic geochemistry, preservation of the record. In *Earth's Earliest Biosphere: Its Origin and Evolution* (ed. J. W. SCHOPF), pp. 93–134. Princeton Univ. Press.

HUTCHINSON C. S. (1974) *Laboratory Handbook of Petrographic Techniques.* Wiley-Interscience.

JACOBSEN S. B. and PIMENTEL-KLOSE M. R. (1988) A Nd isotopic study of the Hamersley and Michipicoten Banded Iron Formations: The source of REE and Fe in Archean Oceans. *Earth Planet. Sci. Lett.* **87,** 29–44.

JAMES H. L. (1954) Sedimentary facies of iron-formation. *Econ. Geol.* **49,** 235–294.

JAMES H. L. (1955) Zones of regional metamorphism in the Precambrian of northern Michigan. *Geol. Soc. Amer. Bull.* **66,** 1455–1488.

KLEIN C., JR. (1974) Greenalite, stilpnomelane, minnesotaite, crocidolite and carbonates in a very low-grade metamorphic Precambrian iron-formation. *Canadian Mineral.* **12,** 475–498.

KLEIN C. (1983) Diagenesis and metamorphism of Precambrian banded iron-formations. In *Iron-Formation: Facts and Problems* (eds. A. F. TRENDALL and R. C. MORRIS), pp. 417–465. Elsevier.

KLEIN C. and BEUKES N. J. (1989) Geochemistry and sedimentology of a facies transition from limestone to iron-formation deposition

in the early Proterozoic Transvaal Supergroup, South Africa. *Econ. Geol.* **84,** 1733–1774.

KLEIN C. and BRICKER O. P. (1977) Some aspects of the sedimentary and diagenetic environment of Proterozoic banded iron-formation. *Econ. Geol.* **72,** 1457–1470.

KLEIN C. and FINK R. P. (1976) Petrology of the Sokoman Iron Formation in the Howells River area, at the western edge of the Labrador Trough. *Econ. Geol.* **71,** 453–487.

LECHLER P. J., ROY W. R., and LEININGER R. K. (1980) Major and trace element analysis of 12 reference soils by inductively coupled plasma-atomic emission spectrometry. *Soil Sci.* **130,** 238–241.

MACLEOD W. N. (1966) The geology and iron deposits of the Hamersley Range area. *Geol. Surv. W. Aust. Bull* **117.**

MIYANO T. (1987) Diagenetic to low-grade metamorphic conditions of Precambrian iron-formations. In *Precambrian Iron-Formations* (eds. P. W. UITTERDIJK APPEL and G. L. LABERGE), pp. 155–186. Theophrastus Publications, S. A.

MIYANO T. and BEUKES N. J. (1984) Phase relations of stilpnomelane, ferri-annite, and reibeckite in very low-grade metamorphosed iron-formations. *Trans. Geol. Surv. S. Africa* **87,** 111–124.

MÜLLER G., SCHUSTER A., and HOEFS J. (1986) The metamorphic grade of banded iron-formations: Oxygen isotope and petrologic constraints. *Fortschr. Mineral.* **64,** 163–185.

PERRY E. C. (1983) Oxygen isotope geochemistry of iron-formation. In *Iron Formation: Facts and Problems* (eds. A. F. TRENDALL and R. C. MORRIS), pp. 359–372. Elsevier.

PERRY E. C., TAN F. C., and MOREY G. B. (1973) Geology and stable isotope geochemistry of the Biwabik Iron Formation, Northern Minnesota. *Econ. Geol.* **68,** 1110–1125.

ROSENBAUM J. and SHEPPARD S. M. F. (1986) An isotopic study of siderites, dolomites, and ankerites at high temperatures. *Geochim. Cosmochim. Acta* **50,** 1147–1150.

SANTROCK J., STUDLEY S. A., and HAYES J. M. (1985) Isotopic analyses based on the mass spectrum of carbon dioxide. *Anal. Chem.* **57,** 1444–1448.

SCHIDLOWSKI M., HAYES J. M. and KAPLAN I. R. (1983) Isotopic inferences of ancient biochemistries: Carbon, sulfur, hydrogen, and nitrogen. In *Earth's Earliest Biosphere: Its Origin and Evolution* (ed. J. W. SCHOPF), pp. 149–185. Princeton Univ. Press.

SHAPIRO L. (1975) Rapid analysis of silicate, carbonate, and phosphate rocks—revised edition. *US Geol. Surv. Bull.* **1401,** 76p.

SHEPPARD S. M. F. and SCHWARCZ H. P. (1970) Fractionation of carbon and oxygen isotopes and magnesium between coexisting metamorphic calcite and dolomite. *Contrib. Mineral. Petrol.* **26,** 161–198.

THORNE A. M. (1983) Upward-shallowing sequences in the Precambrian Duck Creek Dolomite, Western Australia. *Geol. Surv. W. Australia Prof. Pap., 1983,* pp. 81–93.

TRENDALL A. F. (1973) Iron-formations of the Hamersley Group of Western Australia: Type examples of varved Precambrian evaporites. In *Genesis of Precambrian Iron and Manganese Deposits,* pp. 257–280. Unesco, Earth Sciences.

TRENDALL A. F. and BLOCKLEY J. G. (1970) The iron formations of the Precambrian Hamersley Group, Western Australia, with special reference to the associated crocidolite. *Geol. Surv. W. Australia Bull.* **119,** 366 pp.

TRENDALL A. F. and PEPPER R. S. (1977) Chemical composition of the Brockman Iron Formation. *Geol. Surv. W. Australia Rec. No. 1976/25.*

VEIZER J. (1983) Chemical diagenesis of carbonates: Theory and application of trace element technique. In *Stable Isotopes in Sedimentary Geology* (eds. M. A. ARTHUR et al.), Chap. 3, pp. 3–100. Soc. Paleon. and Mineralogists, Short Course No. 10.

WALKER J. C. G. (1984) Suboxic diagenesis in banded iron formations. *Nature* **309,** 340–342.